

Anomalous $E1$ and $E2$ strengths in ^{40}Ca and ^{48}Ca at low excitation energy: A comparative study

S. Ottini-Hustache,^{1,*} N. Alamanos,¹ F. Auger,¹ B. Castel,² Y. Blumenfeld,³ V. Chiste,¹ N. Frascaria,³ A. Gillibert,¹
C. Jouanne,³ V. Lapoux,¹ F. Marie,¹ W. Mittig,⁴ J. C. Roynette,³ and J. A. Scarpaci³

¹DSM/DAPNIA/SPhN, CEA/Saclay, F-91191 Gif-sur-Yvette Cedex, France

²Department of Physics, Queen's University, Kingston, Ontario, Canada K7L 3N6

³IPN Orsay, IN2P3-CNRS, F-91406 Orsay Cedex, France

⁴GANIL, B.P. 5027, F-14076 Caen Cedex 5, France

(Received 16 September 1998)

We present the results of an experimental comparative study of the $^{40,48}\text{Ca}$ resonance spectra between 6 and 12 MeV. The power of the heavy ion reaction $^{40,48}\text{Ca}(^{86}\text{Kr}, ^{86}\text{Kr}')^{40,48}\text{Ca}^*$ at 60 MeV per nucleon was exploited to enhance greatly the low energy part of inclusive spectra in order to look for the possible presence of a low energy dipole mode in ^{48}Ca due to a neutron skin. We did not observe any difference in the $l=1$ channel and therefore found no evidence of this mode. In the $l=2$ channel, an important excess of strength was observed in ^{40}Ca compared to ^{48}Ca . [S0556-2813(99)05306-6]

PACS number(s): 24.10.Eq, 24.30.Gd, 25.70.De, 27.40.+z

To what extent does the addition of eight neutrons modify the structure of ^{48}Ca compared to the doubly magic ^{40}Ca ? Are these modifications, if any, likely to affect also the collective observables like giant resonances? These are important questions in nuclear structure especially in light of the current interest generated by neutron halo low energy vibration modes expected to occur in unstable neutron-rich nuclei. In ^{48}Ca , the precursor of such phenomena could be seen as an out-of-phase oscillation of the $f_{7/2}$ neutrons against the $N=Z=20$ core. This would manifest itself as a decoupling of the $E1$ strength from the GDR and appear as a small low energy $l=1$ resonance. Several years ago, Harvey and Khanna studied the occurrence of enhanced low energy resonances in ^{208}Pb and showed that their strength and position would be sensitive markers of the parameters of the nuclear force [1]. More recently, Chambers *et al.* [2] used the RPA in the density functional method to predict the occurrence in neutron rich calcium isotopes of a "soft" $E1$ resonance. The calculated transition density shows the onset of such a "soft" $E1$ mode whose strength would increase linearly with neutron number, its largest signal standing at around 8 MeV in ^{48}Ca and exhausting about 5% of the $E1$ EWSR. Since all RPA calculations predicted the onset of the GDR to be seen well above 15 MeV in both isotopes, the position and strength of the weaker $E1$ resonance in ^{48}Ca should be visible in a comparison of $l=1$ spectra of ^{40}Ca and ^{48}Ca since it should not appear in the ^{40}Ca spectrum.

A similar comparison in the $l=2$ channel is also very interesting. Indeed, experimental results for ^{40}Ca are scattered: measured strengths of the GQR mainly stand around 50% of the EWSR but can vary up to 80% [3-7]. This is anyway low compared to conventional RPA calculations which predict that this resonance exhausts almost 100% of the EWSR, with the same structure in both ^{40}Ca and ^{48}Ca

with a centroid at $E=16$ MeV and half-width of about 5 MeV (there is thus no theoretical basis to expect the occurrence of such a large spreading width in calcium). Recently, Kamerdzhev *et al.* [8] have suggested that effects beyond RPA, like ground state correlations induced by particle-hole-phonon coupling would redistribute some of the $E2$ strength to lower energy and produce a splitting of the familiar GQR. In ^{48}Ca one would expect ground state correlations to be of a different nature than in ^{40}Ca , leading there to a different distribution of quadrupole strength.

Thus, in both $l=1$ and $l=2$ channels, a comparative study of the ^{40}Ca - ^{48}Ca spectra is likely to yield interesting insight in the structure of giant resonances and their low energy manifestations. It is the purpose of this Brief Report to present results of such an investigation.

Heavy ion inelastic scattering is a very efficient tool to investigate low excitation energy states. Indeed, the strong Coulomb excitation provided by a high energy and high Z projectile results in an enhancement of the very low energy part of the excitation cross section [9,10]. For instance, for $E1$ transitions the differential cross section can be written as

$$\frac{d^2\sigma}{d\Omega dE} = \left(\frac{d^2\sigma}{d\Omega dB(E1)} \right)_E b_{E1}(E)\uparrow,$$

where $[d^2\sigma/d\Omega \cdot dB(E1)]_E$ is the DWBA cross section evaluated at excitation energy E for unit excitation strength, $B(E1)\uparrow = 1 \text{ e}^2\text{fm}^2$. This cross section represents the pure Coulomb excitation generated by the colliding nuclei for uniform transition strength. The nuclear response to this solicitation is introduced via $b_{E1}(E)\uparrow = dB(E1)\uparrow/dE$, the distribution of $E1$ reduced matrix element per unit energy, which can be related to the photonuclear cross section $\sigma_\gamma(E)$ by

$$b_{E1}(E)\uparrow = \frac{9\hbar c}{16\pi^3} \frac{\sigma_\gamma(E)}{E}.$$

*Present address: GANHIL, B.P. 5027, F-14076 Caen Cedex 5, France.

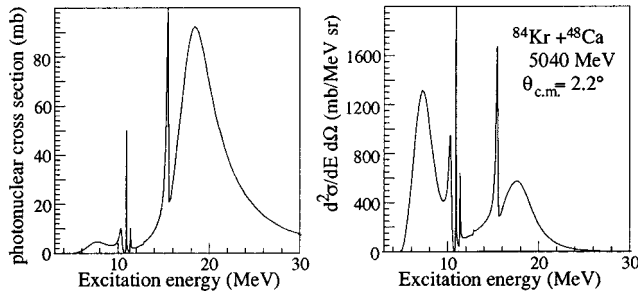


FIG. 1. Comparison between a photoabsorption spectrum calculated by Chambers *et al.* [2] (left side) and a calculation using these results combined with the Coulomb excitation probability for the reaction $^{84}\text{Kr}(^{48}\text{Ca}, ^{48}\text{Ca}^*)^{84}\text{Kr}$ at 60 MeV per nucleon (right side) at an angle of 2.2° in the center of mass frame.

The Coulomb excitation probability is a decreasing exponential function of excitation energy. As an example, the effect of the combination of the photoabsorption spectrum and the Coulomb excitation probability is shown in Fig. 1 in the case of $^{84}\text{Kr} + ^{48}\text{Ca}$ inelastic scattering. The left part shows the results of Chambers *et al.* [2] for the photonuclear cross section in ^{48}Ca . The broad resonance around 8 MeV is the ‘‘soft’’ $E1$ resonance mentioned above, exhausting about 5% of the EWSR. The right part is a calculation using these results combined with the formalism described above, for the $^{84}\text{Kr}(^{48}\text{Ca}, ^{48}\text{Ca}^*)^{84}\text{Kr}$ reaction at 60 MeV/nucleon at an angle of 2.2° in the center of mass frame. The results are striking in that one observes that the photoabsorption spectrum is greatly distorted by the diffusion with krypton, the low energy part of the spectrum being ‘‘amplified’’ with respect to the high energy side. The cross section of the ‘‘soft’’ resonance becomes even more important than the usual GDR’s one, centered around 19 MeV. This demonstrates the power of the inelastic scattering of heavy ions for the study of low excitation energy transitions, such as the soft $E1$ resonance.

Therefore, we have performed an experiment at GANIL, with a ^{86}Kr beam at 60 MeV/nucleon impinging on two thin (about 0.5 mg/cm^2) targets of ^{40}Ca and ^{48}Ca . The targets were fabricated, transported and installed in the scattering chamber under vacuum, to avoid any oxydization. There was no detectable impurity. The scattered ^{86}Kr , in the charge state 35^+ , were detected and identified in the high resolution spectrometer SPEG, in which their scattering angle and energy were measured with an accuracy of 0.2° and 1.4 MeV ($\Delta E/E = 2.7 \times 10^{-4}$), respectively. The spectrometer was centered at 2.2° in the laboratory frame, covering an angular range from 0.3° to 4.2° . The elastic and low energy inelastic scattering were partly suppressed by insertion of movable absorbers before the focal plane. The excitation energy was measured from about 5 MeV as can be seen on Fig. 2, and up to several hundreds of MeV. The spectra shown here are not normalized since the targets’ thicknesses were not known precisely and the charge state distribution of the outgoing ^{86}Kr was not measured. Therefore, the absolute normalization of the data was obtained using GDR and GQR results of Ref. [5] for the excitation energy between 13 and 25 MeV (see Fig. 3). We have subtracted a constant background (following the results obtained in [7]) whose angular distribution was assumed to be similar to the angular distribution of the

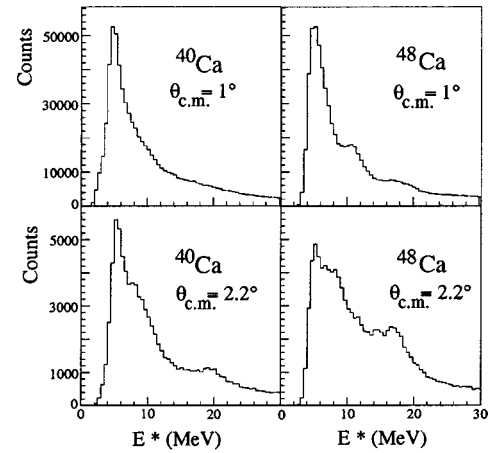


FIG. 2. Excitation energy spectra obtained with ^{40}Ca (left side) and ^{48}Ca (right side) targets, for $0.85^\circ < \theta_{\text{c.m.}} \leq 1.15^\circ$ (upper part) and $2.05^\circ < \theta_{\text{c.m.}} \leq 2.35^\circ$ (lower part) where dipole transitions dominate. The spectra binning is 500 keV.

energy region located immediately above the giant resonances region. The consistency of this normalization method was verified with elastic scattering for the ^{40}Ca target (see Fig. 3), indicating that the strengths measured in [5] are correct within experimental errors. The uncertainty on the absolute normalization is more important for ^{48}Ca , for which data in Ref. [5] are less precise ($89 \pm 27\%$ for ^{48}Ca compared to $86 \pm 11\%$ for ^{40}Ca for the giant quadrupole resonance).

Using these data, we have extracted the $E1$ and $E2$ transition strengths for both targets and for different bins in excitation energy. Since we cannot distinguish between target and projectile excitations, the strengths determined here concern the whole system. But ^{86}Kr excitations show up in the same way with both targets, allowing us to make a compar-

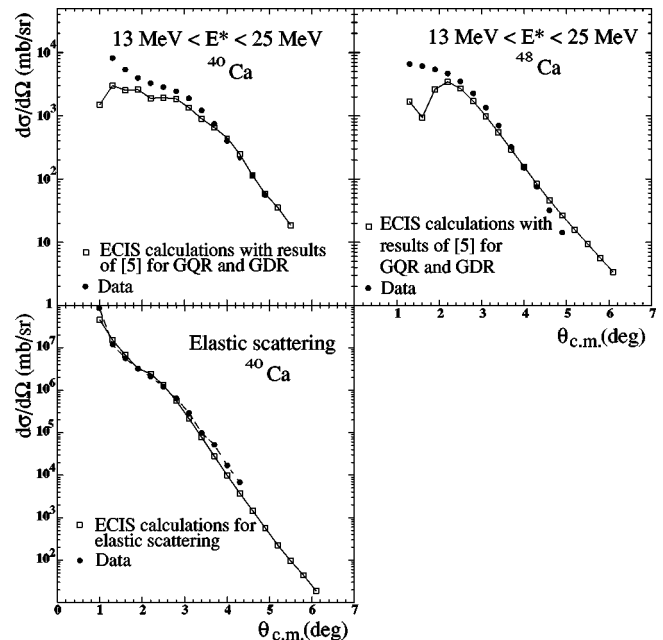


FIG. 3. Absolute normalization of the data (dots) using results of [5] for GQR and GDR for E^* between 13 and 25 MeV (open squares). Comparison of normalized data for elastic scattering on ^{40}Ca with ECIS calculations.

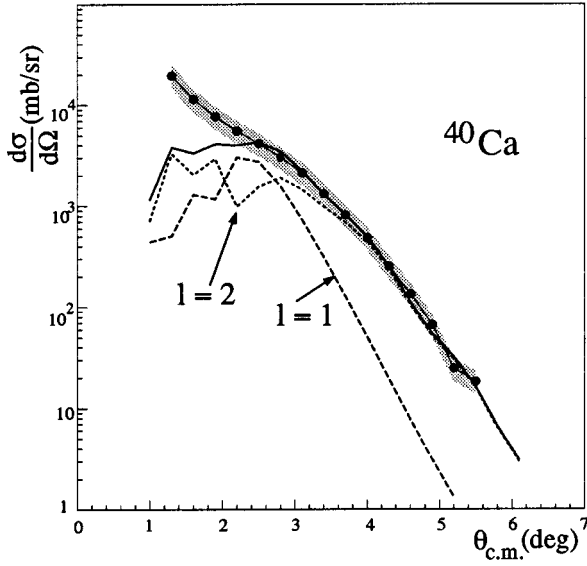


FIG. 4. Angular distribution obtained with the ^{40}Ca target, for $6 \text{ MeV} < E^* < 8 \text{ MeV}$. The grey area represents the uncertainty on absolute normalization. The fit obtained with a coupled channel calculation is indicated by the solid line. The dashed lines respectively represent $E1$ and $E2$ transitions only.

tive study of the calcium isotopes. A typical example is shown in Figs. 4 and 5. The cross section is plotted as a function of scattering angle in the center of mass system for an excitation energy between 6 and 8 MeV for both targets. Since we consider all kind of transitions, collective and single particle ones, and we make a comparative study of both targets, no background was subtracted. The gray area around the data corresponds to the uncertainty on the absolute global normalization factor applied to each point of the angular distribution. The data are fitted with calculations performed with ECIS, in the framework of coupled channels

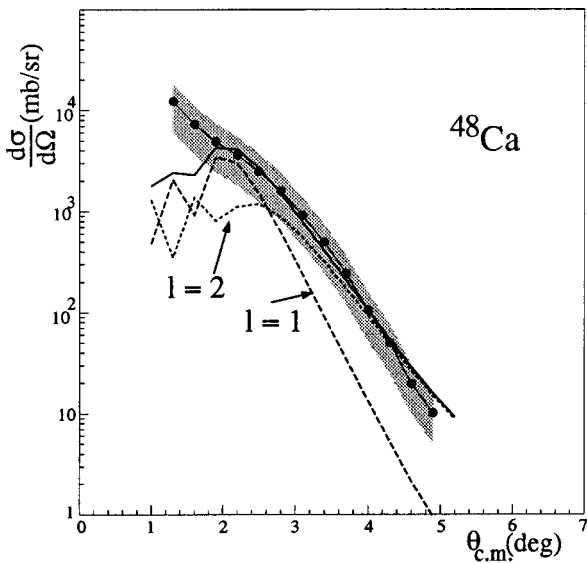


FIG. 5. Angular distribution obtained with the ^{48}Ca target, for $6 \text{ MeV} < E^* < 8 \text{ MeV}$. The grey area represents the uncertainty on absolute normalization. The fit obtained with a coupled channel calculation is indicated by the solid line. The dashed lines respectively represent $E1$ and $E2$ transitions only.

TABLE I. Percentage of the EWSR extracted from the data for $l=1$ and $l=2$ transitions for three energy regions. The errors are determined by the uncertainty on absolute normalization. The error due to multipolarity decomposition is negligible compared to this error. The percentage difference between ^{40}Ca and ^{48}Ca is given in the last column. The total strength between 6–12 MeV cannot be read as the cumulative sum because of the common boundaries. For ^{40}Ca target and for $8 \text{ MeV} \leq E^* \leq 10 \text{ MeV}$ and $10 \text{ MeV} \leq E^* \leq 12 \text{ MeV}$, we have introduced 5% of EWSR for monopole transitions, following the results of [6].

$E(\text{MeV})$	^{40}Ca		^{48}Ca		Difference	
	$l=1$	$l=2$	$l=1$	$l=2$	$l=1$	$l=2$
[6,8]	2.6 ± 0.6	8.3 ± 2.0	3.1 ± 1.5	4.2 ± 2.1	-0.5	+4.1
[8,10]	4.9 ± 1.2	15.6 ± 3.9	3.6 ± 1.8	8.8 ± 4.4	+1.3	+6.8
[10,12]	6.6 ± 1.6	15.8 ± 3.9	7.0 ± 3.5	10.0 ± 5.0	-0.4	+5.7

equations [11], using $E1$ and higher multipolarity electric transitions. These higher multipolarity transitions nevertheless should be dominated by $l=2$ ones and therefore we performed the calculations with quadrupolar transition strength only. It should be noted that any small contribution of higher multipolarity would strongly decrease the strength attributed here to quadrupolar transitions. One can see that the behaviors of the two contributions with scattering angle are very different, allowing to determine the only combination of $l=1$ and $l=2$ cross sections reproducing the data. The relative contribution of each kind of transitions is therefore well determined. The uncertainty on the normalization factor, by far dominating other sources of error (particularly the multipolarity decomposition error), defines the precision on the absolute strength extracted for $l=1$ and $l=2$. The calculations are indeed very close to the experimental values for angles larger than 2.2° . The discrepancy at lower angles probably comes from the elastic scattering of the beam on entrance slits of the spectrometer which stop nuclei up to 0.3° in the laboratory frame. The contribution of this process is very difficult to evaluate. The good agreement between data and calculations from 2.2° in the center of mass (0.8° in the laboratory) indicates that the contribution of this parasitic elastic scattering becomes negligible.

The $E1$ and $E2$ strengths extracted are summarized in Table I. Note that calculations have been done assuming $l=1$ and $l=2$ excitations of the calcium targets only. For ^{40}Ca target and for $8 \text{ MeV} < E^* < 10 \text{ MeV}$ and $10 \text{ MeV} < E^* < 12 \text{ MeV}$, we have introduced 5% of EWSR for monopole transitions, following the results of [6]. For ^{48}Ca , according to Kamerdzhev [12], the monopolar strength in this excitation energy region can be neglected and this difference between the two isotopes is caused by the difference in shell structure of the two nuclei. Above 10 MeV, the strength cannot be attributed to krypton excitations due to neutron emission.

In the $l=1$ case, two general observations come to mind.

(1) One observes non-negligible $E1$ strength with both targets in the low excitation energy region studied here. There is no theoretical basis for such a strength, since all RPA calculations (*with* or *without* ground state correlations) predict no $E1$ strength below 14 MeV in either isotope except in [2] for ^{48}Ca .

(2) We do not observe any $E1$ strength difference between ^{48}Ca and ^{40}Ca . Therefore, there is no evidence of the excitation of a soft dipole mode in ^{48}Ca . Nevertheless, the $E1$ strength observed between 8 and 10 MeV is indeed consistent with the predictions of Chambers *et al.* [2]. A better study of the low excitation energy spectrum of $^{40, 48}\text{Ca}$ could be achieved in the forthcoming years with the improved energy resolution of the new focal plane detection of SPEG. The expected energy resolution of 150 keV would allow to study whether the strength observed in ^{48}Ca possesses the collective features, i.e., resonance shape and transition density, expected for the soft $E1$ mode [2].

The analysis of our $l=2$ data indicates that there is a significant difference between the two targets for $E2$ strength below 12 MeV. One observes a systematic excess of $E2$ strength in each excitation energy bin for ^{40}Ca compared to ^{48}Ca and such an excess is not observed in the $l=1$ case for which there is whether a small lack or excess of strength depending on excitation energy. This shows that the $l=2$ strength is not affected by a systematic error, since the relative contribution of each multipolarity is precisely defined by the shape of the angular distribution. Summing $l=2$ strengths between 6 and 12 MeV, we obtain an excess of

16.7% for ^{40}Ca , which is overestimated because of the common boundaries of energy bins. Therefore, despite the large error bars, we can conclude that there is actually an excess of $E2$ strength of about 15% in ^{40}Ca compared to ^{48}Ca .

As mentioned earlier, this departure from RPA predictions can be explained by invoking the presence in that nucleus of strong ground state correlation effects [8]. There is no indication however *why these mechanisms should be so much weaker in ^{48}Ca as to reduce their contribution by the factor observed here.*

In conclusion, the results of our experiment using a particularly powerful and efficient probe for detecting low-lying excitations suggest that, in the $E1$ and $E2$ cases, our theoretical understanding of collective excitations should be critically reassessed. This is becoming especially important as higher resolution facilities are coming on line which will further test our understanding of the microscopic structure of collective excitations, as well as their coupling to more complex degrees of freedom.

The authors would like to thank J. Barrette for many fruitful discussions and for his very careful reading of this paper. They are also grateful to D.H. Youngblood for discussions and communication of his data.

[1] M. Harvey and F. C. Khanna, Nucl. Phys. **A221**, 77 (1974).

[2] J. Chambers *et al.*, Phys. Rev. C **50**, 2671 (1994).

[3] A. Van der Woude, Prog. Part. Nucl. Phys. **18**, 217 (1987).

[4] J. Lisantti *et al.*, Phys. Rev. C **40**, 211 (1989).

[5] F.T. Baker *et al.*, Phys. Rev. C **44**, 93 (1991).

[6] D.H. Youngblood *et al.*, Phys. Rev. C **55**, 2811 (1997).

[7] J.A. Scarpaci *et al.*, Phys. Rev. C **56**, 3187 (1997).

[8] S. Kamenarzhiev, J. Speth, and G. Tertuchuy, Phys. Rev. Lett. **74**, 3943 (1995).

[9] J. Barrette *et al.*, Phys. Lett. B **209**, 182 (1988).

[10] J.R. Beene *et al.*, Phys. Rev. C **41**, 920 (1990).

[11] J. Raynal, Phys. Rev. C **23**, 2571 (1980).

[12] S. Kamenarzhiev *et al.*, Nucl. Phys. **A577**, 641 (1994).